

Oscillating Fracture Paths in Rubber

Robert D. Deegan, Paul J. Petersan, M. Marder, and Harry L. Swinney

Center for Nonlinear Dynamics and Department of Physics, The University of Texas at Austin, Austin, Texas 78712

(Received 6 July 2001; published)

We have found an oscillating instability of fast-running cracks in thin rubber sheets. A well defined transition from straight to wavy cracks occurs as the amount of biaxial strain increases. Measurements of the amplitude and wavelength of the oscillation near the onset of this instability indicate that the instability is a Hopf bifurcation.

DOI:

PACS numbers: 62.20.Mk, 81.05.Lg, 83.60.Uv, 89.75.Kd

When a balloon is pricked, a crack races around it, slicing the material into fragments. Surprisingly, instead of running straight the crack wiggles, leaving a wavy pattern on the edges of the fragments. This effect has likely been observed before, but we have found only one documented case [1]. We have constructed an experiment to study this phenomenon. The wavy pattern is the result of a straight-running crack losing stability to a new state in which the crack oscillates about its mean direction of motion.

The field of dynamic fracture was spawned by theoretical attempts to understand why straight-running cracks in brittle materials bifurcate [2]. Despite the great advances in dynamic fracture since then [3], predicting the path of a rapidly moving crack is beyond the current theory. Here we report the first experiments showing that a crack moving at speeds comparable to the speed of sound can spontaneously begin to oscillate. This phenomenon is different from the branching instability because biaxial strain is essential, and therefore studying this phenomenon provides a new avenue to attack the larger issue of crack path selection.

The applicability of fracture mechanics to elastomers has been established [4–6], the time-dependent characteristics of elastomer fracture have been examined [7,8], and crack speeds under varying degrees of biaxial strain have been investigated [9,10]. None of these studies, however, has explored the transition from a straight to a wavy crack path. Our aim here is to characterize this instability.

Our experiments were done with flat sheets of rubber in biaxial tension. We used samples taken from a single roll of 0.18 mm thick natural latex sheet (100% cis-polyisoprene [11]). Our apparatus, inspired by a similar technique developed by Treloar [12], is shown in Fig. 1. Tabs were prepared on 32.5 cm \times 12.7 cm sheets by cutting 1.2 cm long slots, perpendicular to the edge, 2.5 cm apart [Fig. 1(a)]. The tips of these incisions were rounded by melting them with a soldering iron to prevent cracks from initiating at these points during loading of the sample.

The experiment proceeds by gripping the tabs and incrementally increasing the load simultaneously in both x and y directions until the desired strain level is reached. The applied strain is on the order of 200%, uniform within

5%, and always chosen so that the strain in the y direction, ϵ_y , is greater than the strain in the x direction, ϵ_x . Strain is measured from the dilation of the grid; deviations from uniform strain are identified from the distortion of the grid and minimized by individually adjusting each clamp. Once the desired strain level is attained, the rubber sheet is sandwiched between a pair of 10 cm \times 66 cm rectangular steel frames [Fig. 1(b)]. The loading is then maintained entirely by the frames.

Each run is initiated by pricking the sheet with a pin at the point marked \times in Fig. 1(b). As shown in Fig. 2, the crack tip that forms is sharp and wedge-shaped [13]. The

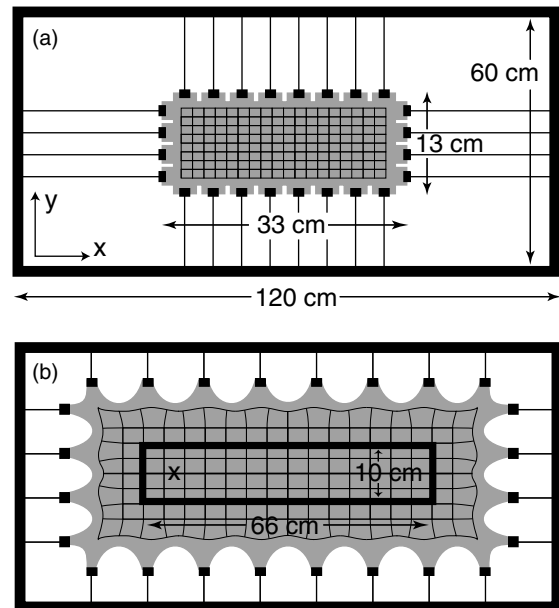


FIG. 1. The experimental apparatus for straining rubber sheets along two axes. (a) A grid is drawn on the sample and clamps are attached to precut tabs along the sample's edges. The load is applied to the sample through the clamps, which are attached by wires to the rigid outer frame. (b) After the sheet has been slowly extended in the x and y directions, it is clamped by an inner rectangular frame. The sheet is distorted near its edges but not inside the inner frame. After clamping the sheet, it is punctured with a pin at the point marked \times . Since the edges of the sheet are clamped, no energy flows into it during fracture.

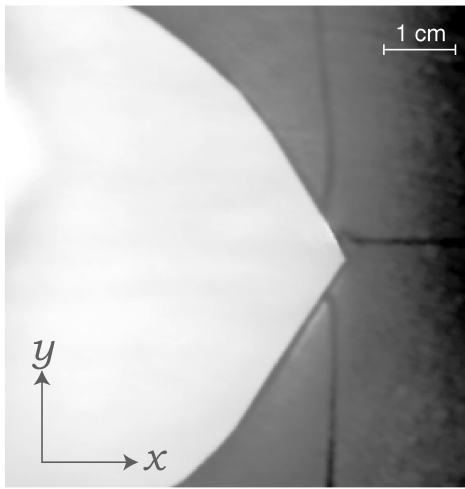


FIG. 2. Snapshot of the tip of a propagating crack. The crack is moving from left to right. The initial conditions were $\epsilon_y = 2.3$ and $\epsilon_x = 1.8$.

crack travels down the centerline, the midpoint between upper and lower edges of the frame.

The speed of the crack, v , depends on the strain state of the sheet. The longitudinal wave speed in the x and y direction, c_x and c_y , also depend on the strain state and are generally not equal. The crack speed, measured by high-speed video, varies between 37 and 60 m/s and is reproducible to within 10%. Over a similar strain range the longitudinal sound speed varies between 54 and 108 m/s $\pm 5\%$ as measured by a time-of-flight method [14]. The ratio v/c_y ranges from 0.4 to 0.6. Since the crack speed is comparable to the speed of sound, the crack propagation is dynamic rather than quasistatic.

Depending on the initial strain conditions, the crack runs straight or oscillates about the centerline. The inner frame makes steady states possible because the energy stored per unit length inside the framed sample is constant ahead of the crack and also constant in its wake. Hence as the crack tip advances it consumes a fixed amount of energy per unit length of advancement. Indeed, we observe that after an initial transient period, an oscillating crack propagates with a wavelength and amplitude that are constant to within 10%.

Examples of the paths of a straight and a wavy crack are shown in Fig. 3. These curves were obtained by scanning the cracked sheet with a flatbed scanner and applying an edge-finding algorithm to the resulting image. Transients typically dominate the first 15% of the crack length. During this transient regime a wavy crack's oscillations grow to saturation and a straight crack recovers from any off-centerline starts, as shown in the inset of Fig. 3(a).

Rubber sheets subjected to different initial strain states were fractured, and the crack path was found to undergo a transition from straight to wavy with increasing biaxial strain. Since the applied forces are purely tensile, the strain state is fully described by ϵ_x and ϵ_y [15]. The results

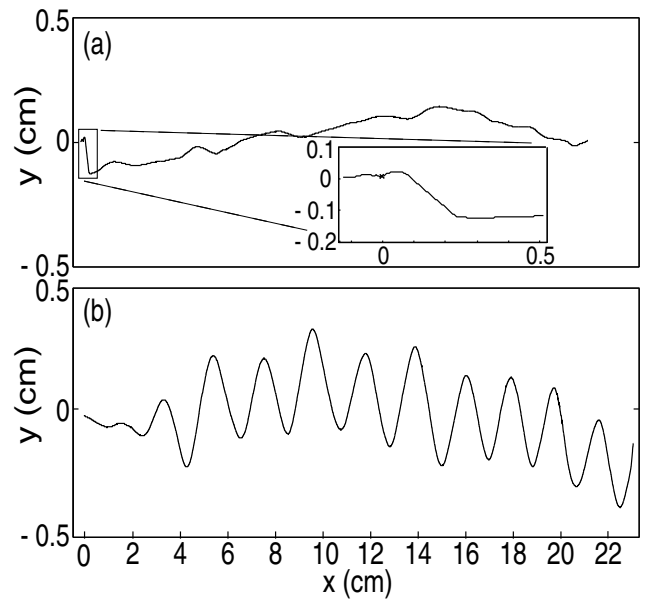


FIG. 3. (a) A straight crack with $\epsilon_x = 1.2$, $\epsilon_y = 2.0$ (inset shows the initial kink that is sometimes observed) and (b) an oscillating crack with $\epsilon_x = 1.3$, $\epsilon_y = 1.8$ are shown in the final, unstrained state. In both cases, the crack initiated at the left edge and propagated to the right.

of these runs are shown in the phase diagram in Fig. 4. The control parameter range was limited by experimental difficulties found at the highest and the lowest values of ϵ_y . For $\epsilon_y > 2.6$ it became impossible to complete a run because cracks would spontaneously form at the high stress point between the tabs. For $\epsilon_y < 1.4$ it became impossible to distinguish between straight and wavy cracks because the wavelength became comparable to the length of the sample, as indicated by the trend in the inset of Fig. 4.

We measured the average wavelength $\langle \lambda \rangle$ and the average amplitude $\langle A \rangle$ of the wavy edge while holding $\epsilon_y = 2.4$ fixed and varying ϵ_x from 1.2 to 2.0. From the digitized curves we extracted the wavelength as the peak-to-peak distance in the x direction and the amplitude as half the peak-to-valley distance in the y direction. These quantities, averaged over multiple runs with the same initial conditions, are plotted in Fig. 5.

The amplitude grows as the square root of the control parameter with a critical value of x strain, $\epsilon_x = 1.36$. Furthermore, if we assume that the crack travels with a constant velocity v in the x direction, then the wavelength is equal to $2\pi v/\omega$, where ω is the frequency at which the crack tip oscillates in the y direction. Since at onset of the instability the wavelength is nonzero, the frequency at onset is nonzero. Hence, we conclude that the observed transition is consistent with a Hopf bifurcation [16,17].

The waveform of the crack path is approximately sinusoidal over a wide range of amplitudes (0.03 to 0.39 cm) and wavelengths (0.56 to 5.0 cm). Figure 6 illustrates this point with two waveforms taken from the runs used to construct Fig. 5. These curves correspond to the first data

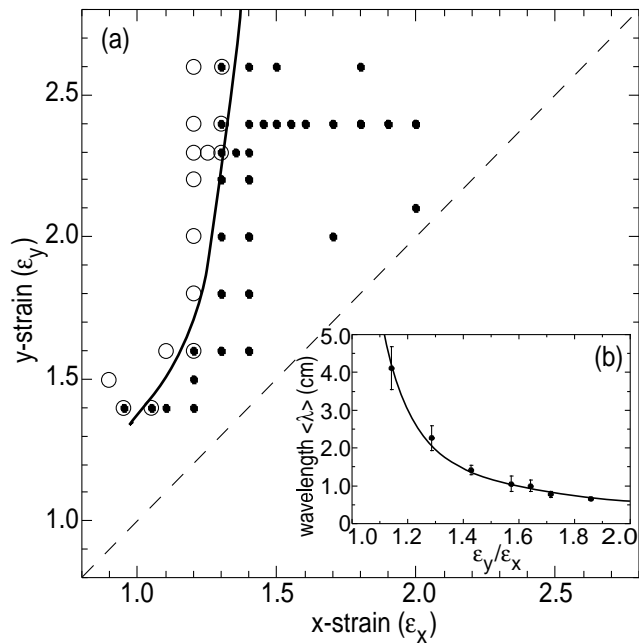


FIG. 4. (a) A phase diagram showing the two observed states: oscillating cracks \bullet , and straight cracks \circ , as a function of the initial strain state, ϵ_x and ϵ_y (frame size = 10 cm \times 66 cm). The solid line, drawn to guide the eye, shows the phase boundary between straight and wavy cracks. Data were not taken in the region below the dashed line because there the principal direction of crack motion is across the width of the frame. Ambiguous points \odot appear at high values of ϵ_y because different runs with the same initial conditions produced both straight and wavy cracks; ambiguous points at low values of ϵ_y result from the difficulty in discriminating between straight and wavy cracks. (b) Wavelength versus ϵ_y , normalized by ϵ_x , for fixed $\epsilon_x = 1.4$. The solid line is a fit of the data to $A/(\epsilon_y/\epsilon_x - 1)$, which yields $A = 0.58$.

point after the transition and the last data point in Fig. 5. The waveform near the transition is almost a perfect sinusoid, further bolstering the identification of the transition as a Hopf bifurcation. The waveform far from the transition shows sizable deviations from a sinusoid; it is skewed in the direction of propagation.

In addition to our quantitative results, we explored the possibility that the oscillation arises from out-of-plane vibrations, strain crystallization, and interaction of the crack tip with waves reflected from the boundary. In one experiment we reduced out-of-plane motion by sandwiching the rubber sheet snugly between two glass plates after the sheet was stretched to the loaded state. In another experiment we loaded the sheet as usual and then forced a cylindrical surface into the sheet so that the sheet was everywhere pressed into contact with the surface; thus, the only out-of-plane motion possible was away from the surface. Neither experiment stopped the crack from oscillating; hence out-of-plane motion is not the source of crack oscillations.

We also considered the effect of strain crystallization, which is the propensity of aligned polymer chains to form

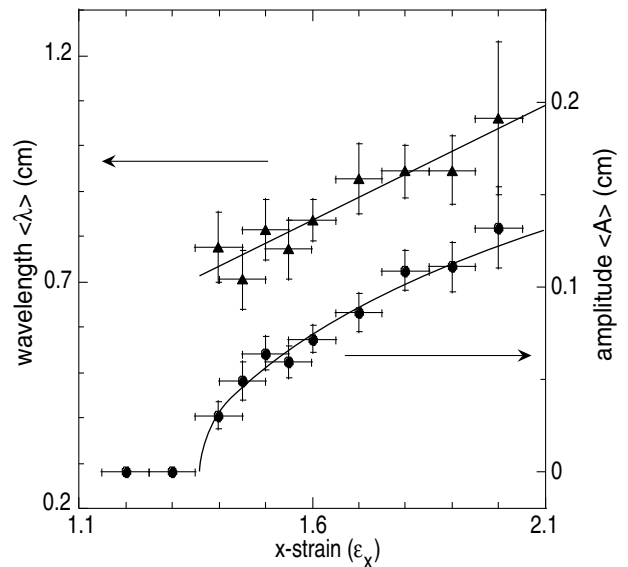


FIG. 5. Amplitude $\langle A \rangle$ (\bullet) and wavelength $\langle \lambda \rangle$ (\triangle) are plotted across the transition from straight to oscillating cracks ($\epsilon_y = 2.4$; see Fig. 4). The solid line through the amplitude data is a square root fit.

crystalline domains that locally stiffen the material [12]. Since natural rubber is well known to strain crystallize, we tested thin sheets of nitrile rubber (a cross-linked copolymer of butadiene and acrylonitrile), which do not strain-crystallize [18]. We found that wavy cracks were nonetheless produced in nitrile; this indicates that strain crystallization is not the source of the instability.

In brittle materials, waves originating from the crack tip and reflecting from the boundaries produce periodic markings such as those identified as Wallner lines [19]. If such a mechanism were active in rubber, one would expect an

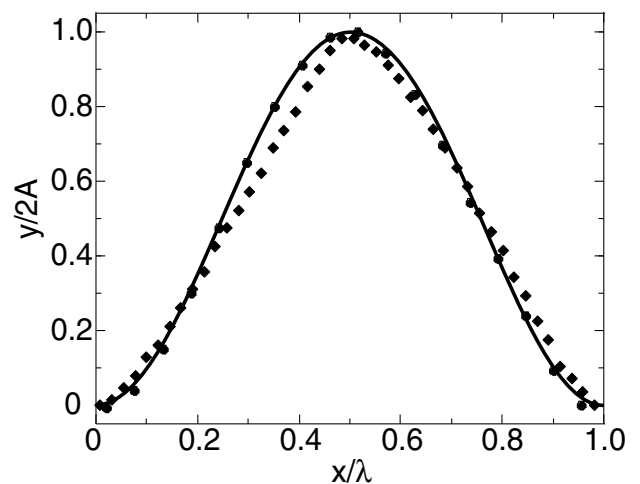


FIG. 6. Profiles of individual peaks from two different runs are scaled by their amplitude and wavelength and plotted together. A sine curve (solid line) is plotted for comparison. (\bullet : $\epsilon_x = 1.4$, $\epsilon_y = 2.4$, $A = 0.03$ cm, $\lambda = 0.75$ cm; \blacklozenge : $\epsilon_x = 2.0$, $\epsilon_y = 2.4$, $A = 0.13$ cm, $\lambda = 1.02$ cm).

oscillatory wavelength $\lambda = (2h\nu/c)/\sqrt{1 - \nu^2/c^2}$, where h is the distance to the boundary. Given that the vertical boundary is 5 cm from the crack and that our measurements show $\nu/c > 0.4$, it follows that $\lambda > 4$ cm. Yet, we observe wavelengths down to 0.85 cm (in the strained state). Thus waves reflecting from the boundary cannot account for the oscillations of the crack.

In conclusion, we have found an instability in the direction of crack propagation in a rubber sheet: subjected to sufficient biaxial strain the crack will oscillate about its mean direction of propagation. We have shown that this instability can be characterized as a Hopf bifurcation. We have ruled out strain crystallization, out-of-plane motion, and wave reflections from the boundary as possible mechanisms for the oscillation.

We are grateful to Stefan Luding for introducing us to this phenomenon and to Gyu-Seung Shin for assistance. We thank Eric Gerde, Matt Lane, W.D. McCormick, L. Mahadevan, and Eran Sharon for helpful discussions, the National Science Foundation for support under DMR-9802562, and the Vice President for Research at the University of Texas at Austin for an exploratory grant.

[1] A. Stevenson and A. Thomas, *J. Phys. D* **12**, 2101 (1979).
 [2] E. Yoffe, *Philos. Mag.* **42**, 739 (1951).
 [3] L. Freund, *Dynamic Fracture Mechanics* (Cambridge University Press, Cambridge, 1998).
 [4] A. Thomas, *Rubber Chem. Technol.* **67**, G50 (1994).
 [5] G. Lake, *Rubber Chem. Technol.* **68**, 435 (1995).
 [6] C. Extrand and A. Gent, *Int. J. Fract.* **48**, 281 (1991).
 [7] A. Kadir and A. Thomas, *Rubber Chem. Technol.* **54**, 15 (1981).
 [8] G. Lake, A. Samsuri, S. Teo, and J. Vaja, *Polymer* **32**, 2963 (1991).

[9] A. Gent and P. Marteny, *J. Mater. Sci.* **17**, 2955 (1982).
 [10] G. Lake, C. Lawrence, and A. Thomas, *Rubber Chem. Technol.* **73**, 801 (2000).
 [11] The force-extension curve for our sample in simple extension follows a Mooney-Rivlin force law up to an extension ratio of $\xi = L/L_o = 5.8$, where L is the extended length and L_o is the relaxed length. Above this extension ratio the modulus increases abruptly due to the finite-length polymer chain effects. A fit to the low-strain data yields $C_1 = 124$ kJ/m³ and $C_2 = 174$ kJ/m³ for the coefficients in the Mooney-Rivlin energy density $e = C_1(\sum_{i=1}^3 \xi_i^2 - 3) + C_2(\sum_{i=1}^3 1/\xi_i^2 - 3)$ (energy per unit of unstrained volume) [12].
 [12] L. Treloar, *The Physics of Rubber Elasticity* (Clarendon Press, Oxford, 1975).
 [13] This shape is different from the parabola of conventional fracture theory [3]. The differences arise from the large deformations present in the material and from the nonlinear constitutive relation for rubber.
 [14] The longitudinal wave speed was obtained by plucking the sheet in-plane and measuring the travel time between two transducers.
 [15] We attempted to parametrize the transition with the energy release rate, i.e., the energy needed to create a unit area of new surface, calculated as $G = [e(\xi_x, \xi_y) - e(\xi_x, 1)]h_o$ where h_o is the width of the sheet before it is loaded. By itself the energy release rate is insufficient to characterize the transition because along the phase boundary G varies from 200 to 320 kJ/m². Attempts to find a second variable to remove this degeneracy produced diagrams with an ill-defined phase boundary.
 [16] A. Yuse and M. Sano, *Nature (London)* **362**, 329 (1993).
 [17] M. C. Cross and P. C. Hohenberg, *Rev. Mod. Phys.* **65**, 851 (1993).
 [18] S. Bhattacharjee, A. K. Bhowmick, and B. N. Avasthi, in *Elastomer Technology Handbook*, edited by N. P. Cheremisinoff (CRC Press, Boca Raton, Florida, 1993).
 [19] B. Lawn, *Fracture of Brittle Solids-Second Edition* (Cambridge University Press, Cambridge, U.K., 1993).